Dynamical Insights into Extreme Short-Term Precipitation Associated with Supercells and Mesovortices

Erik R. Nielsen and Russ S. Schumacher

Department of Atmospheric Science, Colorado State University, Fort Collins, CO

INTRODUCTION

- Rotation on various scales (e.g., supercells and MCVs is often associated with extreme rainfall (see Smith et al. 2001, Schumacher and Johnson 2009, Hitchens and Brooks 2013).
- In other research by the authors, observed rain rates over 75 mm/hr are associated with mesoscale rotation nearly half of the time (e.g., Fig. 1)
- Various mechanisms can lead to rotation, including precipitation processes in the cases of MCV development (e.g., Raymond and Jiang 1990) and tilting of environmental vorticity in the case of supercells (e.g., Markowski and Richardson 2014)
- Low-level shear can have an important influence on storm characteristics, evolution, and the development of rotation (e.g., Nowotarski et al. 2011, Coffer and Parker 2015)
- Vertical perturbation pressure gradient forces (VPPGF) associated with rotation can serve to enhance dynamical lifting in the presence of rotation (Eqn. 1)
- It is hypothesized that mesoscale rotation can aide in maximizing rain rates by dynamically enhancing the updraft and lifting otherwise negatively buoyant parcels that contain moisture and instability

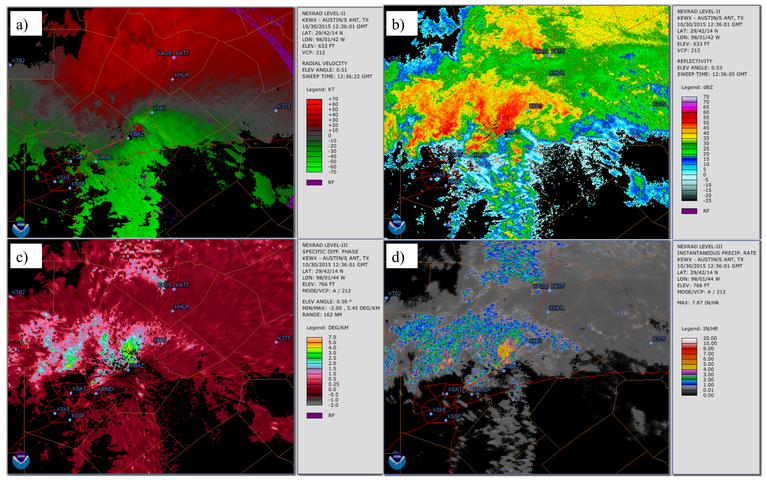

Fig. 1: *Radial Velocity (a), reflectivity (b), specific differential phase (KDP, c), and instantaneous precipitation rain rate (d) from the Austin/San Antonio, TX (KEWX) WSR-88D radar valid 30 October 2015 at 12:36 UTC.*

DATA AND METHODS

- Idealized, numerical simulations were conducted in CM1 (Bryan and Fritsch 2002) based upon the kinematic profile of the event depicted in Fig. 1 in south-central Texas where hourly rainfall accumulations of 100 to 177 mm were seen
- In addition to the simulation based upon the kinematic profile of the above event (CONTROL, Fig. 2b-c), two additional simulations were conducted using wind profiles with weaker low-level shear, but similar hodograph shape (LOW_SHEAR, MED_SHEAR, Fig. 2d,e, respectively), since the primary purpose of these experiments is to explore how changes in the magnitude of the low-level wind shear affects storm dynamics and precipitation production
- The initial homogenous environmental thermodynamic profile for all simulations (Fig. 2a) was taken from extreme rainfall composite of Schumacher and Johnson (2009)
- Buoyant and dynamic components of the vertical perturbation pressure gradient force will be numerically solved for each run following the methods of Parker and Johnson (2004) and Coffer and Parker (2015)

$$\frac{\partial w}{\partial t} = \underbrace{\vec{v}\cdot\nabla_h w}_{\text{Advection}} \underbrace{- \frac{1}{\rho_0}\frac{\partial p_B'}{\partial z}}_{\text{Total Buoyant Acc. (ACCB)}} \underbrace{- g\frac{\rho'}{\rho_0}}_{\text{Buoyancy (B)}} \underbrace{- gq_h}_{\text{Drag}} \underbrace{- \frac{1}{\rho_0}\frac{\partial p_{DL}'}{\partial z}}_{\text{Nonlinear Dynamic Acc. (NLD-VPPGF)}} \underbrace{- \frac{1}{\rho_0}\frac{\partial p_{DNL}'}{\partial z}}_{\text{Linear Dynamic Acc.}} \quad (1)$$

For More Information Contact: Erik.Nielsen@colostate.edu

Numerical Model Results

Questions to investigate:

How do changes in the magnitude of the low-level shear vector affect storm dynamics and precipitation production?

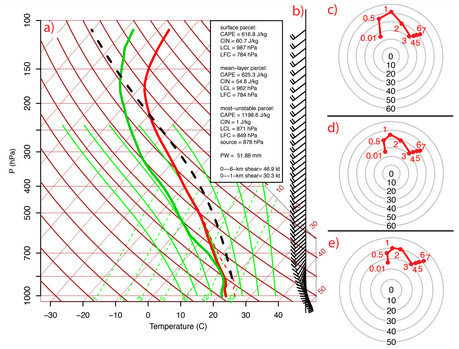

Fig. 2: *(a) Composite thermodynamic profile from Schumacher and Johnson (2009). Hodographs (kt) of wind profile used for wind 0–1km shear sensitivity experiments for CONTROL (c), MED SHEAR (d), and LOW SHEAR (e) cases derived from CSU-WRF model sounding valid 1500 UTC 30 October 2015 near San Antonio, TX. (b) wind profile corresponding to control hodograph (c).*

- The three simulations produce convective systems that are similar in size, shape, and speed (Fig. 3)
- Low-level rotation develops in all three simulations but is strongest and most sustained in the highest shear run (CONTROL, Fig. 3) and weakest in the lowest shear run (LOW_SHEAR)
- Robust, storm scale cold pools develop by the end of both the MED_SHEAR and LOW_SHEAR simulations (not shown)
- The average low-level vertical motion is larger and sustained for a longer period of time in the CONTROL run compared to the other simulations (not explicitly shown)

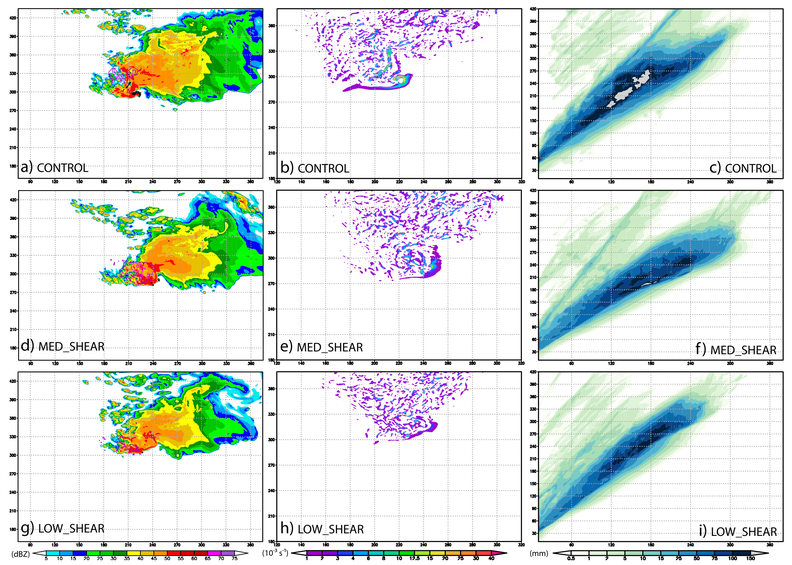

Fig. 3: *(a,d,g) Simulated 1 km radar reflectivity (shaded; every 5 dBZ from 5dBZ to 70 dBZ), surface perturbation potential temperature (Θ; contoured at -1.5 and -2.5 K in dark purple and magenta, respectively), and contoured 1 km vertical vorticity (black contours) valid t=11 h into the simulations for the (a) CONTROL, (d) MED_SHEAR, (g) LOW_SHEAR simulations. (b.e.h) Corresponding 1 km vertical vorticity ($10^{-3}s^{-1}$) for the (b) CONTROL, (e) MED_SHEAR, (h) LOW_SHEAR simulations. (c,f,i) run total accumulated precipitation (mm) for run corresponding to left two columns.*

Statistic	Control	Med_Shear	Low_Shear
Mean Areal Accumulation (mm km^{-2})	3.10	2.43	1.95
Max Accumulation (mm)	220	167	142
Coverage of at least 25 mm Accumulation	5.66%	5.05%	3.88%
Coverage of at least 50 mm Accumulation	3.75%	2.90%	2.36%
Coverage of at least 100 mm Accumulation	1.19%	0.42%	0.36%
Coverage of at least 150 mm Accumulation	0.27%	0.02%	N/A
Coverage of at least 200 mm Accumulation	0.009%	N/A	N/A

Table 1: *Modeled rainfall accumulation statistics.*

- **Substantially more precipitation** occurred in terms of point maximum , areal mean, and areal coverage of large accumulations for the CONTROL run compared to the MED_SHEAR and LOW_SHEAR simulation (Table 1)
- The CONTROL run regularly produces stronger maximum updrafts in the lowest 2 km (e.g., 20 m/s at 500m and 40 m/s at 1.5 km) compared to the other two runs (not shown)
- All three convective systems are able to ingest parcels from the convectively inhibited lower levels (not shown)

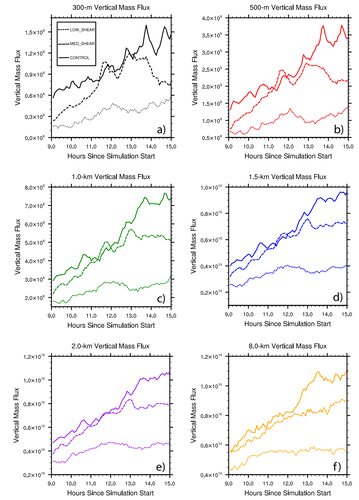

Fig. 4: *Total vertical mass flux (g/s) of updrafts with magnitude greater that 1 m/s over the portion of the domain shown in Fig. 3 at (a) 300 m, (b) 500 m, (c) 1.0 km, (d) 1.5 km, (e) 2.0 km, and (f) 8 km for the CONTROL (solid line), MED_SHEAR (dashed line), and LOW_SHEAR (dotted line).*

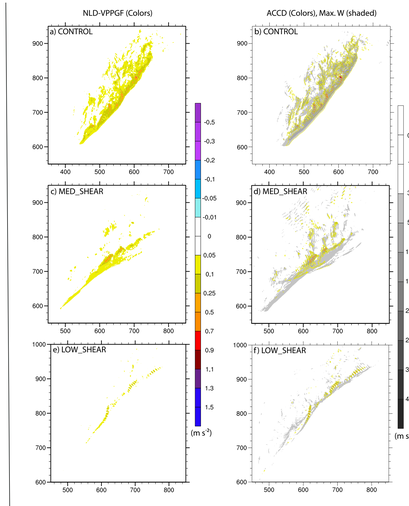

Fig. 5: *(a,c,e) translated swaths of maximum dynamic nonlinear vertical perturbation gradient acceleration (m/s^2) for the labeled runs. (b,d,f) translated swath of maximum 500 m vertical velocity (shaded, m/s) with 500 m maximum total dynamic acceleration (ACCD) overlaid in same colors intervals as (a,c,e).*

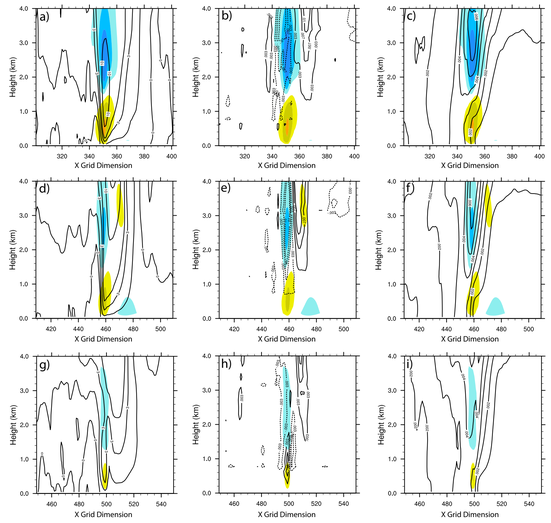

Fig. 6: *Time mean east-west cross sections through the point of maximum 500 m NLD-VPPGF acceleration (fill contour, m/s^2) overlaid with mean vertical velocity (left column, m/s), total buoyant accelerations (middle column, m/s^2), and total condensate mixing ratio (right column, g/kg) for CONTROL (top row), MED_SHEAR (middle row), and LOW_SHEAR (bottom row).*

- Large differences are seen in low-level positive vertical mass flux (Fig. 4), where the vertical mass flux at each level ordered to the amount of low-level shear in each simulation (i.e., more shear, more mass flux)
- Increase low-level vertical accelerations associated with the rotational term of the VPPGF are seen in runs with increase shear and rotation (cf. color fill Fig. 5a,c,e)
- Rotational induced dynamic accelerations dominate over other dynamic accelerations in the low levels (cf. Fig. 5a,c,e to b,d,f)
- Higher sustained mean vertical motion is seen in the lowest levels in higher shear runs (Fig. 6a,d,g) associated with dynamic accelerations
- Buoyant accelerations are, comparatively, an order of magnitude weaker at these levels (Fig. 6 b,e,h)

CONCLUSIONS and ACKNOWLEDGEMENTS

- In conclusion, precipitation systems in intense 0—1 km shear that develop mesoscale rotation can aide in producing extreme precipitation by enhancing the magnitude of the low-level updrafts through accelerations associated with rotationally induced non-linear dynamic vertcal perturbation pressure gradient forces.
- The resulting increase in low-level vertical motion can further serve to enhance precipitation, depending on the environmental conditions, by ingesting otherwise negatively buoyant parcels that still contain moisture and CAPE.
- Provides a potential explanation for the observed frequency of concurrent, collocated tornado and flash flood events (i.e., TORFFs, Nielsen et al. 2015).

- This research was supported by National Science Foundation Grant AGS-1359727, NOAA grants NA15OAR4590233 and NA16OAR4590215, and a National Science Foundation Graduate Research Fellowship Grant DGE-1321845, Amendment 3. The authors would like to thank Matthew Parker, Brice Coffer, Stacey Hitchcock, Greg Herman, and John Peters for helpful commentary on this work.